

# Optimal Configuration of a Downward-Facing Monocular Camera for Visual Odometry

Mohammad O. A. Aqel<sup>1\*</sup>, Mohammad H. Marhaban<sup>1</sup>, M. Iqbal Saripan<sup>2</sup>,  
Napsiah Bt. Ismail<sup>3</sup> and Asem Khmag<sup>2</sup>

<sup>1</sup>Department of Electrical and Electronic Engineering, Faculty of Engineering, Universiti Putra Malaysia, UPM, 43400 Serdang, Selangor, Malaysia; aqel2001@hotmail.com, mhmm@upm.my

<sup>2</sup>Department of Computer and Communication Engineering, Faculty of Engineering, Universiti Putra Malaysia, UPM, 43400 Serdang, Selangor, Malaysia; iqbal@upm.edu.my, khmaj2002@gmail.com

<sup>3</sup>Department of Mechanical and Manufacturing Engineering, Faculty of Engineering, Universiti Putra Malaysia, UPM, 43400 Serdang, Selangor, Malaysia; napsiah@upm.edu.my

## Abstract

**Background/Objectives:** An accurate estimation of a robot's pose is critical for autonomous mobile vehicles. Monocular vision-based odometry is one of the robust methods used for estimating the relative motion of vehicles by using only a stream of images acquired from a camera mounted on the vehicle. **Methods:** The location of the camera and its configuration can affect the quality of the localization process and the maximum permissible vehicle driving speed. In this work, the elements that can affect the permissible vehicle driving speed were recognized and the equations for this allowable speed were derived. Moreover, the optimal location and configuration of a downward-facing monocular camera that ensures the success of Visual Odometry for car-like ground vehicles in low-textured environment are presented after an extensive analysis. **Findings:** The results show that the suggested optimal camera configuration increases the permissible vehicle driving speed. Furthermore, the percentage of correlation mismatching between image frames is decreased as the suggested camera location avoids the negative consequences of shadows and directional sunlight that can add noise to image frames and interrupt the estimation of image pixel displacement. **Application/Improvements:** The suggested camera configuration could be implemented in various commercial mobile robotic applications, which utilize visual odometry for improved accuracy, efficiency and cost effectiveness.

**Keywords:** Camera Configuration, Correlation, Monocular, Permissible Driving Speed, Vision-Based Odometry

## 1. Introduction

For autonomous navigation, a robot must maintain knowledge of its position over time. Different sensors and techniques can be utilized for localization tasks, such as wheel odometry, a Global Positioning System (GPS), an Inertial Navigation System (INS) and visual sensors. However, each technique has its own weaknesses. Although wheel odometry is the simplest technique available for position estimation, it suffers from position drift due to wheel slippage<sup>1,2</sup>. INS is highly prone to accumulating drift and a highly precise INS is expensive and

an unviable solution for commercial purposes<sup>3</sup>. Although GPS is the most common solution to localization as it can provide absolute position without error accumulation, it is only effective in places with a clear view of the sky. Moreover, it cannot be used indoors and in confined spaces<sup>3,4</sup>. The commercial GPS estimates position with errors in the order of meters. This error is considered too large for precise applications that require accuracy in centimeters, such as autonomous parking. Differential GPS and real time kinematic GPS can provide position with centimeter accuracy, but these techniques are expensive.

\*Author for correspondence

A highly accurate alternative solution for estimating the ego-motion of robots that can avoid most of the aforementioned drawbacks is the Visual Odometry (VO). VO is the localization of a robot using only the stream of images acquired from a camera attached to the robot<sup>5</sup>. VO is an inexpensive solution and is not affected by wheel slippage in uneven terrain. Furthermore, VO works effectively in GPS-denied environments. The rate of local drift under VO is smaller than the drift rate of wheel encoders and low-precision INS<sup>6</sup>. Images store large and meaningful information (color, texture, shape, etc.) that is sufficient for estimating the movement of a camera in an environment<sup>3,7</sup>.

VO has been an active research area for many years<sup>8</sup>. Most VO systems fail or cannot work effectively in outdoor environments with shadow, image blur and directional sunlight. In the present work, the developed vision-based odometry system uses a low-cost downward-facing monocular camera oriented toward a low-textured ground (e.g., asphalt, concrete and soil floor) for estimating the position of ground car-like vehicles. The factors affecting the maximum allowable vehicle driving speed are determined to select the optimal configuration of a camera that can ensure the success of the VO system. Furthermore, to avoid the negative effects of shadow and directional sunlight that disturb the calculation of the pixel displacement between consecutive image frames, the camera is installed underneath the testing vehicle. Normalized cross-correlation template matching is used for calculating the image pixel displacement. It is one of the best methods that can work robustly with almost low-texture surfaces and it is invariant to linear brightness and contrast variations<sup>9-13</sup>.

This paper is organized as follows. A literature review is presented in the following section. Section 3 describes the factors affecting the quality of correlation matching to find the optimal location for a camera installation and the factors affecting the maximum allowable vehicle driving speed are distinguished through the derived equations. Section 4 discusses the results of our experiments. The conclusion for this research is presented in Section 5.

## 2. Literature Review

VO is a non-contact method for effectively positioning mobile robots, mainly in outdoor applications<sup>14</sup>. VO provides an incremental online estimation of a vehicle's

position by analyzing the image sequences captured by a camera<sup>4,15</sup>. It provides an inexpensive solution more accurately than conventional localization techniques such as GPS and wheel odometry. This method has a good balance of cost, reliability and implementation complexity<sup>2,4,16</sup>. One of the main limitations of VO systems is mainly related to light and imaging conditions (i.e., direct sunlight, shadow, image blur, etc.)<sup>13,17,18</sup>.

In the existing literature, most of VO methods use either stereo, as implemented by<sup>16,19,20</sup>, or monocular cameras, as applied by<sup>2,4,14,17,18</sup>. A stereo camera requires more effort in calibration than a monocular camera; errors in calibration directly affect the motion estimation process<sup>21</sup>. Therefore, using a monocular camera can mitigate the effect of calibration errors on motion estimation. In the existing literature, most of VO cameras attached to the vehicle are either oriented toward the ground<sup>2,13,14,18</sup> or facing forward. The forward-facing camera provides more information than the downward-facing camera. However, template matching or feature tracking can be disturbed by shadows and dynamic changes in the environment caused by wind and sunlight<sup>22,23</sup>.

In general, the vision-based odometry technique can be approached in two ways: through a feature-based approach or an appearance-based approach<sup>5</sup>. As used by<sup>6,16,24</sup>, the feature-based approach involves extracting image features between sequential image frames and matching or tracking those among the extracted features that are distinctive<sup>16</sup>. As implemented by<sup>2,4,13,17,18</sup>, the appearance-based approach monitors the changes in appearance of the acquired images and the intensity of pixel information therein instead of extracting and tracking features. The commonly used method in this type of approach is the template matching method.

The feature-based approach is suitable for textured scenarios, such as rough and urban environments<sup>4</sup>. However, it may fail in dealing with low-textured environments as insufficient salient features can be detected in these environments<sup>2,4,13</sup>. By contrast, the template matching method is highly appropriate for use in low-textured scenarios<sup>12</sup>. Normalized cross-correlation is the most common and effective method for template matching<sup>10</sup>. It is invariant to contrast and linear brightness variations<sup>11</sup>. In this work given the lack of salient features in low-textured environments, a normalized cross-correlation template matching technique is used rather than a feature-based method.

### 3. Optimal Configuration of the Camera

The directional sunlight, image blur and shadow from static or dynamic objects and the vehicle itself cause non-uniform scene lighting. This non-uniform lighting and image blur may disturb the calculation of image pixel displacements and cause mismatching or false matching in the correlation process.

As mentioned in Section 2, the camera attached to the vehicle could be oriented either toward the ground or facing forward. Although the forward-facing camera can provide more information than the downward-facing camera, a forward-facing camera under low-light conditions requires the surrounding environment to be lighted; possibly requiring more power than the vehicle can provide. Moreover, with the forward-facing camera, the pixel displacement using template matching or feature tracking can be disturbed by shadows and dynamic changes in the environment caused by wind and sunlight. To avoid such problems and to provide uniform lighting, the camera needs to look toward a fully shaded area on the ground over time. The best possible location for the camera that can ensure the aforementioned condition is under the vehicle between either the front wheels or the rear wheels of the vehicle and facing downward toward the ground. This location prevents directional sunlight, shadows and unwanted objects from interfering with the camera view.

In cameras, a slow shutter speed increases the opportunity for image motion blur. Therefore, the camera should operate at a fast shutter speed to minimize image motion blur. However, a fast shutter speed means short

exposure time and decreased light for every image frame, thus resulting in dark image frames. To provide sufficient uniform illumination for the camera, a lighting module with a circular arrangement of Light Emitting Diodes (LED) around the camera is designed and attached to the camera as shown in Figure 1. This module provided sufficient illumination under fast shutter speeds and ensured that the system operated robustly day and night.

In choosing whether to install the downward-facing camera between the front wheels or between the rear wheels of the vehicle, the factors affecting the maximum permissible vehicle driving speed should be determined. After an extensive analysis, the factors were determined as follows:

- Height of the camera from the ground ( $Z_c$ ) that affects the size of the captured ground area.
- Image template window size ( $T_z = T_w \times T_h$ ) that affects the allowable pixel displacement.
- Image template center location ( $T_x, T_y$ ) that affects the allowable pixel displacement.
- Camera frame rate ( $F_r$ ) that affects the number of frames captured per second.
- Focal length ( $f_x, f_y$ ) that affects the size of the captured ground area.

The downward-facing camera can be attached to the vehicle in two configurations. The first configuration maintained the image height ( $I_h$ ) parallel to the direction of longitudinal (forward/reverse) vehicle motion as shown in Figure 2(a). The second configuration maintained the image width ( $I_w$ ) parallel to this motion as shown in Figure 2(b).

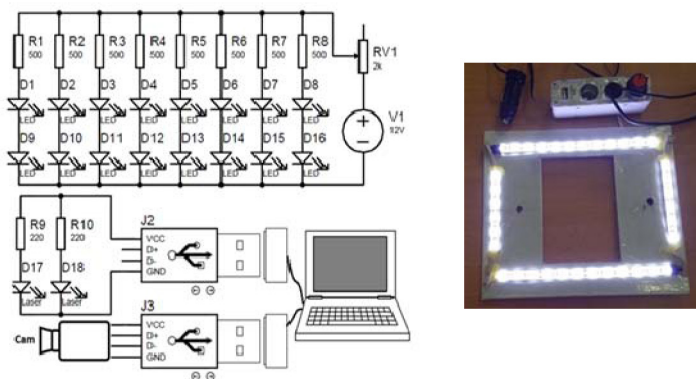


Figure 1. LED lighting module.

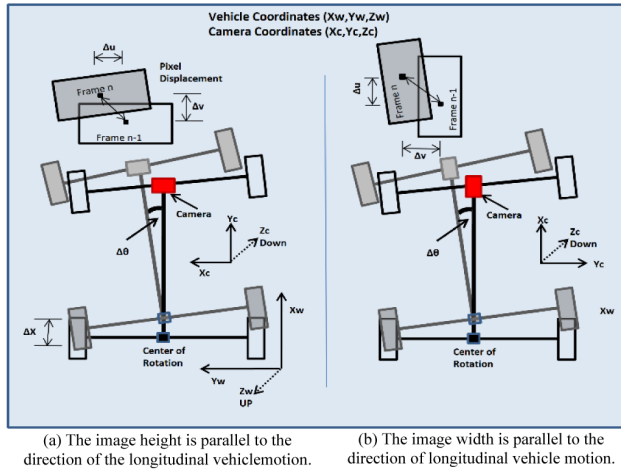


Figure 2. Two configurations of camera installation.

Figure 3 shows how the maximum permissible pixel displacement is to be calculated on the basis of the position of the template and direction of the vehicle motion. As shown in Figure 3(a),  $P_h$  is the allowable pixel displacement per image frame when the camera image height is parallel to the direction of the longitudinal vehicle motion. If the direction of the longitudinal vehicle motion is parallel to the image width instead as shown in Figure 3(b), then the allowable pixel displacement per image frame is represented by  $P_w$  (pixel/frame).  $P_h$  and  $P_w$ , which depend on the size and location of the template, are calculated as:

$$\begin{aligned} P_h &= (I_h - T_y - T_h / 2), \\ P_w &= (I_w - T_x - T_w / 2), \end{aligned} \tag{1}$$

where  $I_h$  and  $T_h$  are the image height and the template height, respectively;  $T_y$  is the vertical template center location;  $I_w$  and  $T_w$  are the image width and the template width, respectively and  $T_x$  is the horizontal template center location.

The calculated allowable pixel displacement in every frame is converted into the physical allowable vehicle displacement (in mm) by conversion from an image coordinate to a camera coordinate system based on the pinhole camera model and using the intrinsic and extrinsic camera calibration parameters as presented in Equation (2).

$$\begin{aligned} V_{h_f} &= P_h \cdot (Z_c / f_y), \\ V_{w_f} &= P_w \cdot (Z_c / f_x), \end{aligned} \tag{2}$$

where  $V_{h_f}$  and  $V_{w_f}$  are the maximum allowable vehicle driving speed in (mm/frame) when the direction of

longitudinal vehicle motion is parallel to the image height and image width, respectively;  $Z_c$  is the camera height from the ground and  $f_x$  and  $f_y$  are the camera horizontal focal length and the vertical focal length, respectively.

To convert the vehicle speed per image frame into the vehicle speed per second, Equation (3) is used.

$$\begin{aligned} V_{h_s} &= V_{h_f} \cdot F_r / 1000, \\ V_{w_s} &= V_{w_f} \cdot F_r / 1000, \end{aligned} \tag{3}$$

where  $V_{h_s}$  and  $V_{w_s}$  are the vehicle speed in m/s when the direction of the longitudinal vehicle motion is parallel to the image height and image width, respectively and  $F_r$  is the camera frame rate per second.

As depicted in Equations (1) to (3), the camera height ( $Z_c$ ) and frame rate have a direct relationship with the maximum allowable driving speed. The camera focal length, template window size and template location have an inverse relationship with the allowable driving speed.

The vehicle motion is estimated by analyzing the image frames and calculating the pixel displacements in the horizontal and vertical directions over time using normalized cross-correlation template matching as it is highly robust for use in low-textured scenarios<sup>12</sup>. For estimating the vehicle motion using a downward-facing monocular camera, some steps are required to be implemented every two consecutive image frames. The estimation cycle process consists of the following steps:

- Calculate pixel displacement between frames in every two consecutive frames.
- Convert pixel image coordinates to camera coordinates.
- Convert pixel displacement to camera displacement in meters.
- Convert camera coordinates to vehicle coordinates.
- Calculate the vehicle displacement (translation and orientation).
- Find the current position of the vehicle in world coordinates.

## 4. Results and Discussion

In this work, several physical experiments were conducted using two monocular cameras to find the optimal location and configuration of the downward-facing camera to be mounted either on the front vehicle bumper

(as in most existing literature) or underneath the vehicle between the front or rear wheels. A Microsoft LifeCam Cinema was used in this work, which has an image frame rate of up to 30 fps and a  $73^\circ$  diagonal field of view. The vehicle used was a Daihatsu Mira L200. The camera calibration toolbox for Matlab developed by Bouguet<sup>25</sup> was used for finding the intrinsic and extrinsic camera parameters.

According to the structure of the vehicle, the camera can be mounted at a higher distance from the ground between the rear wheels (263 mm) than between the front wheels of the vehicle (80 mm). As the camera height from the ground increases, the allowable vehicle driving speed increases as more space area of the ground, which is captured by a higher camera, allows for more pixel displacements between the frames (Figure 3). To choose between the front or the rear vehicle wheels as attachment points for the first camera, the maximum allowable driving speed was calculated at both locations using Equations (1) to (3). For example, when the camera with an image resolution of  $640 \times 480$ , camera focal length of 640 pixels, template size of  $120 \times 120$  and frame rate of 30 fps was mounted between the front wheels at a distance of 80 mm from the ground, the calculated maximum allowable driving speed was less than 1.35 m/s or 1.95 m/s, depending on which image aspect (i.e., either the image width or the image height) was parallel to the direction of the longitudinal vehicle motion. When the camera was mounted between the rear wheels at a height of 260 mm from the ground, the calculated maximum allowable driving speed was approximately 4.40 m/s or 6.35 m/s, depending on

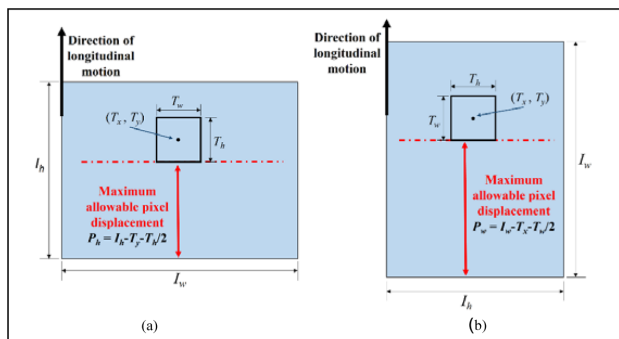


**Figure 3.** Calculation of the maximum permissible pixel displacement based on the location of the template and the motion direction of the vehicle. The direction of the longitudinal vehicle motion is parallel to the image height in (a), while parallel to the image width in (b).



**Figure 4.** Attachment of the cameras to the vehicle. (a) First camera mounted between the rear wheels of the vehicle. (b) Second camera mounted on the front vehicle bumper.

the image aspect parallel to the direction of the longitudinal vehicle motion.

Moreover, we found that when the direction of the longitudinal vehicle motion is parallel to the image width, the obtainable speed is higher than that if the direction of longitudinal vehicle motion is parallel to the image height. This difference is that more pixel displacements can be achieved in the former condition than in the latter. Therefore, the first camera was mounted between the rear wheels of the vehicle instead of between the front wheels (Figure 4(a)). The image width was aligned to be parallel to the direction of the longitudinal vehicle motion. The second camera was mounted on the front vehicle bumper, looking downward at a distance of 370 mm from the ground (Figure 4(b)).

To decide whether the optimal location for the camera was to be mounted on the front vehicle bumper or underneath the vehicle between the rear wheels, a comparison according to the quality of correlation was performed between the two suggested locations. This comparison employed the image sequence frames of video streams in a sunny outdoor environment for several trajectories captured by the two cameras at the same time from an asphalt floor. The vehicle was driven along an S-shaped trajectory, rectangular trajectory and long path trajectory with a total travelled distance of around 150 m, 140 m and 830 m, respectively, as shown in Table 1. The vehicle moved at a speed of 3 m/s to 4 m/s. The image sequences were analyzed. The algorithms were run using Matlab on a computer with Intel(R) Xeon(R) CPU E31225 Quad-core @ 3.1 GHz and 12GB RAM.

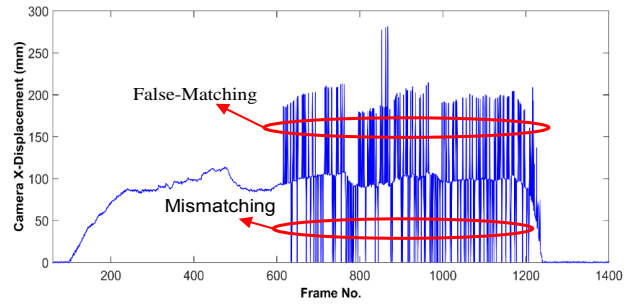
Table 1 shows a comparison of the correlation matching performance between video streams captured using two downward-facing cameras: One mounted on the front vehicle bumper and one mounted between the rear wheels. As shown in Table 1, the camera located between the vehicle’s rear wheels clearly provides a higher quality of correlation matching than the camera mounted on the front vehicle bumper. This location (underneath the vehicle) ensures that the camera is directed toward a fully shaded area and provides a uniform lighting environment without shadow or directional sunlight. This location decreases the opportunity for template correlation mismatching and false-matching.

Figure 5 shows the estimated camera displacement for Camera 1 and Camera 2, in the X-direction for the rectangular-shape trajectory. As shown in Figure 5(a), the displacement estimation of the camera mounted on the front of the vehicle bumper was interrupted by many instances of correlation false-matching and mismatching. By contrast, the displacement estimation of the camera mounted underneath the vehicle did not encounter false-matching or template mismatching, as shown in Figure 5(b).

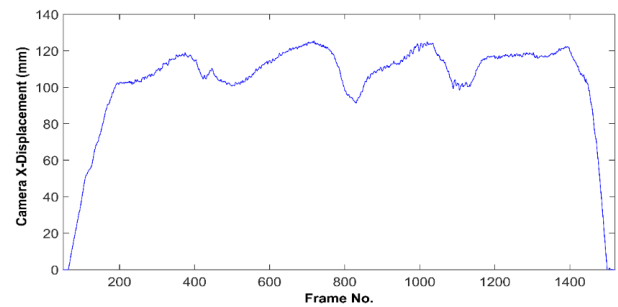
Based on these results, the optimal location for the camera is underneath the vehicle between its rear wheels. Moreover, the best camera configuration is to align the image width to be in parallel to the longitudinal vehicle motion to increase the maximum allowable vehicle driving speed.

Finally, as shown in Table 2, video streams collected from the asphalt floor day and night with and without a light source were compared to check the efficiency of the designed lighting module in providing sufficient uniform illumination day and night at a fast camera shutter speed. This experiment analyzed how the existence of a

light source can improve the quality of the cross-correlation matching process. For videos captured day and night with a light source (Figures 6(a) and 6(c)), a high quality correlation with around 0% mismatching was obtained. By contrast, the quality of the correlation was extremely degraded for videos captured day and night without a light source (Figures 6(b) and 6(d)). The worst case was for the video captured at night without a light source as the



(a) Estimated displacement of the camera mounted on the vehicle bumper.



(b) Estimated displacement of the camera mounted underneath the vehicle.

**Figure 5.** Comparison of the estimated displacement in the X-direction between cameras 1 and 2 for a rectangular trajectory.

**Table 1.** Quality of correlation matching is affected by the location of camera. Camera 1 is located underneath the vehicle between its rear wheels. Camera 2 is located on the vehicle front bumper

Trajectory	Number of frames	Average correlation	Number of mismatching	Number of false matching
S-shape (Cam 1)	1,259	0.906	0	0
S-shape(Cam 2)	1,150	0.886	34	97
Rectangular-Shape (Cam 1)	1,537	0.889	0	0
Rectangular-Shape (Cam 2)	1,423	0.865	79	111
Long path (Cam 1)	8,636	0.946	6	0
Long path (Cam 2)	8,512	0.823	245	1,143

**Table 2.** Existence of a light source improves the quality of correlation matching

Scenario	Number of frames	Average correlation	Number of mismatching
Day, without light source	1,291	0.839	52
Day, with light source	1,190	0.881	0
Night, without light source	1,783	0.368	1,129
Night, with light source	1,741	0.878	2

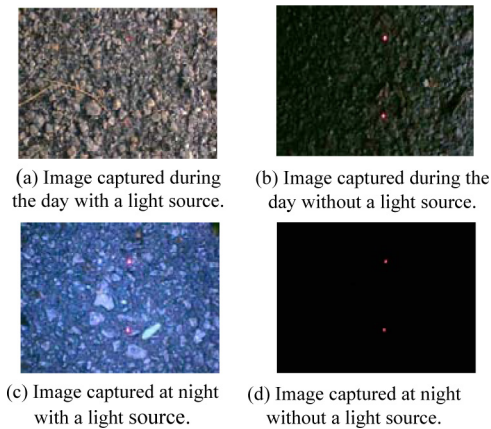


**Figure 6.** Designed lighting module provides sufficient lighting for images captured from an asphalt floor at high shutter speed day and night.

images were almost completely dark. According to Table 2, the template mismatching rate increased when no sufficient illumination was provided.

## 5. Conclusion

This paper presented the factors affecting the quality of correlation-based matching in monocular Visual Odometry. The factors affecting the maximum allowable vehicle driving speed were also determined and the related equations were derived. After an extensive analysis, the optimal location and configuration of the downward-facing monocular camera that could ensure the success of VO was found to be underneath the vehicle between its rear wheels and supported with a lighting module. The results show that at this location, the percentage of cor-

relation mismatching and false-matching between image frames decreases. The suggested camera location avoids the negative effect of directional sunlight and shadow that can add noise to image frames and disturb the calculation of the image pixel displacement. Moreover, the suggested optimal camera configuration, which is to align the image width rather than the image height to be parallel to the longitudinal motion, increases the allowable vehicle travelling speed.

## 6. References

1. Fernandez D, Price A. Visual Odometry for an outdoor mobile robot. 2004 IEEE Conference on Robotics, Automation and Mechatronics; 2004 Dec 1-3. p. 816–21.
2. Nourani-Vatani N, Roberts J, Srinivasan MV. Practical Visual Odometry for car-like vehicles. ICRA'09. IEEE International Conference on Robotics and Automation; Kobe. 2009 May 12-17. 3551–7.
3. Rone W, Ben-Tzvi P. Mapping, localization and motion planning in mobile multi-robotic systems. *Robotica*. 2013 Jan; 31(1):1–23.
4. Gonzalez R, Rodriguez F, Guzman JL, Pradalier C, Siegwart R. Combined Visual Odometry and visual compass for off-road mobile robots localization. *Robotica*. 2012 Oct; 30(6):865–78.
5. Scaramuzza D, Fraundorfer F. Tutorial: Visual Odometry. *IEEE Robotics and Automation Magazine*. 2011 Dec; 18(4):80–92.
6. Howard A. Real-time stereo Visual Odometry for autonomous ground vehicles. IEEE/RSJ International Conference on Intelligent Robots and Systems, IROS; Nice. 2008 Sep 22-26. p. 3946–52.
7. Kundukulam EJ, Sudharson A. Implementing and optimizing template matching techniques for home automation. *Indian Journal of Science and Technology*. 2015 Aug; 8(19):1–6.
8. Wang C, Zhao C, Yang J. Monocular odometry in country roads based on phase-derived optical flow and 4-DOF ego-motion model. *Industrial Robot: An International Journal*. 2011; 38(5):509–20.
9. Mahmood A, Khan S. Correlation-coefficient-based fast template matching through partial elimination. *IEEE Transactions on Image Processing*. 2012 Apr; 21(4):2099–108.
10. Zhao F, Huang Q, Gao W. Image matching by normalized cross-correlation. *ICASSP 2006 Proceedings. IEEE International Conference on Acoustics, Speech and Signal Processing*; 2006. p. 729–32.
11. Zhao F, Huang Q, Gao W. Image matching by multiscale oriented corner correlation. *Computer Vision-ACCV 2006. Springer*. 2006; 3851:928–37.

12. Kicman P, Narkiewicz J. Concept of integrated INS/visual system for autonomous mobile robot operation. *Marine Navigation and Safety of Sea Transportation: Navigational Problems*. 2013 Jun ;35–40.
13. Nourani-Vatani N, Borges PVK. Correlation-based Visual Odometry for ground vehicles. *Journal of Field Robotics*. 2011 Sep; 28(5):742–68.
14. Nagatani K, Ikeda A, Ishigami G, Yoshida K, Nagai I. Development of a Visual Odometry system for a wheeled robot on loose soil using a telecentric camera. *Advanced Robotics*. 2010; 24(8-9):1149–67.
15. Campbell J, Sukthankar R, Nourbakhsh I, Pahwa A. A robust Visual Odometry and precipice detection system using consumer-grade monocular vision. *IEEE International Conference on Robotics and Automation*; 2005 Apr 18-22. p. 3421–7.
16. Nistér D, Naroditsky O, Bergen J. Visual Odometry for ground vehicle applications. *Journal of Field Robotics*. 2006 Jan; 23(1):3–20.
17. Gonzalez R, Rodriguez F, Guzman JL, Pradalier C, Siegwart R. Control of off-road mobile robots using Visual Odometry and slip compensation. *Advanced Robotics*. 2013; 27(11):893–906.
18. Yu Y, Pradalier C, Zong G. Appearance-based monocular Visual Odometry for ground vehicles. *IEEE/ASME International Conference on Advanced Intelligent Mechatronics*; Budapest. 2011 Jul 3-7. p. 862–7.
19. Azartash H, Banai N, Nguyen TQ. An integrated stereo Visual Odometry for robotic navigation. *Robotics and Autonomous Systems*. 2014 Apr; 62(4):414–21.
20. Golban C, Istvan S, Nedeveschi S. Stereo based Visual Odometry in difficult traffic scenes. *Intelligent Vehicles Symposium (IV)*; Alcala de Henares. 2012 Jun 3-7. p. 736–41.
21. Kitt BM, Rehder J, Chambers AD, Schonbein M, Lategahn H, Singh S. Monocular Visual Odometry using a planar road model to solve scale ambiguity. *Proceedings of European Conference on Mobile Robots*; 2011 Sep. p. 1–6.
22. Piyathilaka L, Munasinghe R. An experimental study on using Visual Odometry for short-run self localization of field robot. *5th International Conference on Information and Automation for Sustainability (ICIAFs)*; Colombo. 2010 Dec 17-19. p. 150–5.
23. Dille M, Grocholsky B, Singh S. Outdoor downward-facing optical flow odometry with commodity sensors. *Field and Service Robotics*. Springer Berlin Heidelberg. 2010; 62: 183–93.
24. Benseddik HE, Djekoune O, Belhocine M. SIFT and SURF performance evaluation for mobile robot-monocular Visual Odometry. *Journal of Image and Graphics*. 2014 Jun; 2(1): 7–6.
25. Bouguet J. Camera Calibration Toolbox for Matlab. 2014. Available from: [http://www.vision.caltech.edu/bouguetj/calib\\_doc/index.html](http://www.vision.caltech.edu/bouguetj/calib_doc/index.html)